



ILJS-24- 020

Neotectonic activities around the Benin-Owena basin, Nigeria

Bamisaie¹ O. A. and Olayiwola² K. O.

¹Department of Applied Geology, School of Earth and Mineral Sciences (SEMS), Federal University of Technology, PMB 704 Akure, Nigeria.

²Department of Remote sensing and GIS, School of Earth and Mineral Sciences (SEMS), Federal University of Technology, PMB 704 Akure, Nigeria.

Abstract

The topographic break around Ore, Benin City, and Auchi was studied to provide information about the tectonic evolution that can be inferred from the structures, geomorphology and drainage basin morphology. Some morphotectonic analyses utilized are basin elongation ratio, hypsometric integral, drainage basin asymmetry, valley floor width to valley height ratio, longitudinal profiles, stream length gradient index, and mountain front sinuosity. This study focused on the indicators that can be used to provide information on the timing of the fault-related topographic break. The study also reveals a non-uniform state of tectonic activity within this region. The evolutionary influence of river meanders, faceted spurs, sediment deposits, horst and graben structures were also investigated. The analysis of morphotectonic indices in the drainage basins suggests that the architecture is strongly altered by the prevalent regional structures and lithology. The existing tectonic state of some of these structures varies from active in the northern parts and along the topographic break to slightly active in the southern parts with a minor influence of lithology and the impact of climate change.

Keywords: Morphotectonic indices; River Basin; Tectonics; Topographical break; Triangular facets; Flooding

1. Introduction

Drainage configuration is continuously shaped and influenced by geological structures (emanating from deformational activities), and climate change, such as excess runoff and flooding (Koroknai et al., 2020; Ezati and Gholami, 2022). Anthropological effects on the area under investigation are negligible because such effects are minimal and restricted. This is because the characteristics of river systems are influenced by the development and geometry of active folds and faults and other geologic structures (Gugliotta and Saito, 2019).

This study examines the correlation between tectonic activity and the morphology of the rivers within the Benin-Owena River basin, in the southwestern parts of Nigeria. Tectonic geomorphology explains the gradual modification of river morphologies to prevalent tectonics, along faults and valley floors during uplift and subsidence. This research explores the impact of deformational activity on the relief and morphology of rivers, and the impact of these on the fluvial process rate, sediment load, as well as river size. These influence the fluvial morphological

response to active tectonics (Singh et al., 2018). Active tectonic dictates the river channels and fluvial architecture, the influence of fold and fault development (Baruah et al., 2020; Misra et al., 2020; Pant et al., 2020). Rivers can adjust to existing geological structures (by navigating the paths and openings created by such structures) and to both erosional and cultural changes in response to climatic conditions. Global warming leads to excessive precipitation and flooding. This disrupts river adjustment, resulting in devastating floods in the deltas and downstream. The river system under consideration links the headwaters in the mountainous areas around Okitipupa and Ore (composed mainly of Basement rocks) to the deltas around Benin City and Mahin, downstream to the coastal seas. The bedrock consists of quartzites, schists, granites, gneisses, and migmatites that outcrop as N-S trending elongated bands.

All the areas under investigation (i.e., Ondo, Edo, Ekiti, and Ogun) are high flood areas, as predicted by NiMet (2023). Generally, the wet periods present the greatest threat due to frequent flooding. However, minimal floodings occur in basins with large valley widths. The water flow within a basin is also influenced by slope, and the volume of sediments in suspension (Scorpio and Comiti, 2024).

Major and subtle morphological changes in stream channels that can be linked with neotectonic activities can be carefully analyzed to get information about the tectonic evolution and neotectonic activity of river basins (Ambili and Narayana, 2014; Anand and Pradhan, 2019; Baruah et al., 2020; Misra et al., 2020; Pant et al., 2020). Drainage systems track the development and growth of folds as they respond to changes in surface slope (Fillon et al., 2013). Even the lowest-order streams mimic the landforms, making the stream network an excellent substitute indicator of the organization of the landforms (Fryirs and Brierley, 2012). The morphological indices of eleven sub-basins in the Benin River Basin will be investigated to determine the neotectonic distribution. According to Bull and McFadden (2020) tectonic geomorphology describes the inter-relationship between surface processes and tectonics usually aimed at solving tectonic problems. For structural geology, tectonic activity, and geomorphology, Remote Sensing (RS) and Geographical Information Systems (GIS) are excellent applications. RS and GIS are significant instruments for figuring out tectonics movement from topographic models (DEMs). DEMs are extremely helpful not only for topographic, lithological, landscape, and landform analyses but also for modeling surface processes (Sharma and Kujur, 2012; Radaideh and Mosar, 2019; Shit et al., 2022). To study the morphological situation at the time of formation of the structural break, we relied on tectonic structures and drainage patterns exhibited at the surface. Rivers adapt to prevailing geological (based on composition-brittle or ductile) and structural (cleavages, joints, veins, microstructures-faults and folds) influences (Tandon and Sinha, 2022). This inherent influence will determine the impact of subsequent tectonic activities on geomorphology. This study will also investigate the effects of tectonics on the evolution of triangular facets along faulted landscapes by evaluating the relationships between triangular facet geometry (i.e., width, height and slope) and fault slip. These tectonic interactions of faults and the variations in triangular facet geometry along fault systems can be used as a basis for identifying pre-linked fault segment boundaries along active faults. However, the possibility of retrieving past and on-going movement information from their geometry and configuration is most often overlooked (Tucker et al., 2020). The development of a faceted spur will entail progressive displacements that extend over time, eventually forming horst-like features bounding by graben (commonly associated with extensional fault zones).

2. Geology of the Area

The Dahomey basin extends from offshore through the coast area and inland. It runs from the offshores of Gulf of Guinea landwards through Ghana, Togo and Republic of Benue to Nigeria. The portion of the Dahomey Basin that extends to Nigeria forms a large miogeoclinal wedge that runs from Ghana's Volta delta to Okitipupa Ridge (Okpoli and Eyitoyo, 2016), which is east of Lagos. The western coast in the Nigeria portion of the Dahomey basin is made up of more than 2000 m pile of Cretaceous to recent sediments (Figure 1). The sediment thickness increases landwards from the sea (Azañón et al., 2015). The basin's structural components can be used to describe its physiography. The Benin and Anambra basin is separated by the Okitipupa hinge line while the Niger Delta Basin occupies the southwestern part of the hinge line.

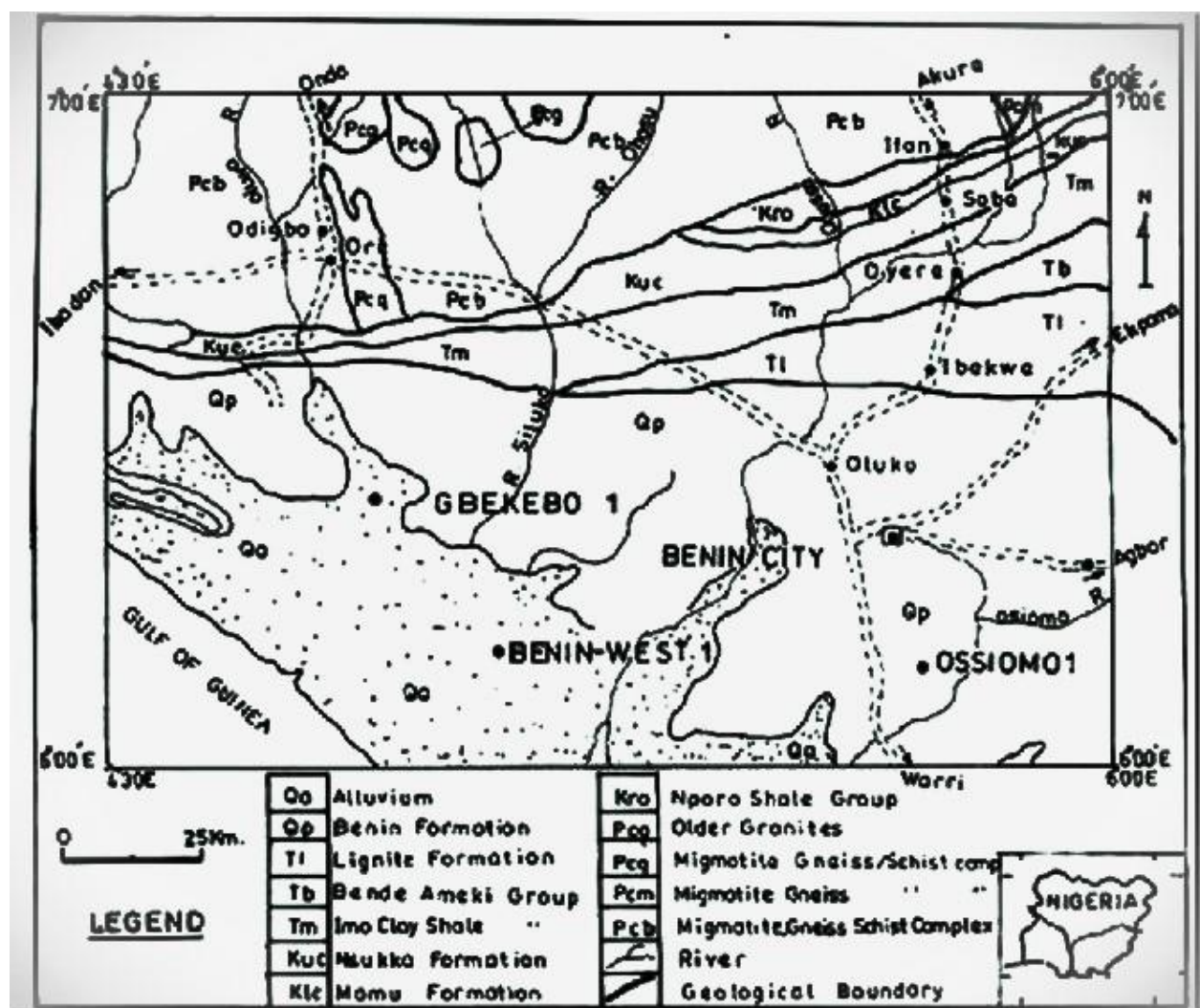


Figure 1: Geological Map of the Benin River basin (Opara et al., 2012)

2.1 Regional structure and tectonics

The Romanche Fracture Zone from the sea, extends to the Ghana Ridge, which forms a boundary with the Benin basin (Dahomey Embayment) in the west (Opara et al., 2012). It is bounded on the east by the Benin Hinge line, which is a basin escarpment that separates the Okitipupa structure from the Niger delta basin (Figure 1 and 2). This marks the continental extension that separates the African–South American landmasses. The subsequent opening of the Atlantic Ocean led to the formation of the sedimentary basin known as the Benin basin during the Mesozoic. It extends from east of Ghana, through Togo and Benin, to western Nigeria, the basin is the onshore portion of the West African geocline. A high and uniform rate of subsidence within the Eastern Dahomey basin was reported by Olabode (2015) during the (Campanian to Maastrichtian period). This represents the earliest formation of the Basin, since the Basin must have been formed before the onset of sediment deposition. Early Cretaceous rifting, dominated by normal faulting and half grabens, was said to be responsible for the basin formation. The major structures here were formed between the early Cretaceous and late Cretaceous (Oladele and Ayolabi, 2014).

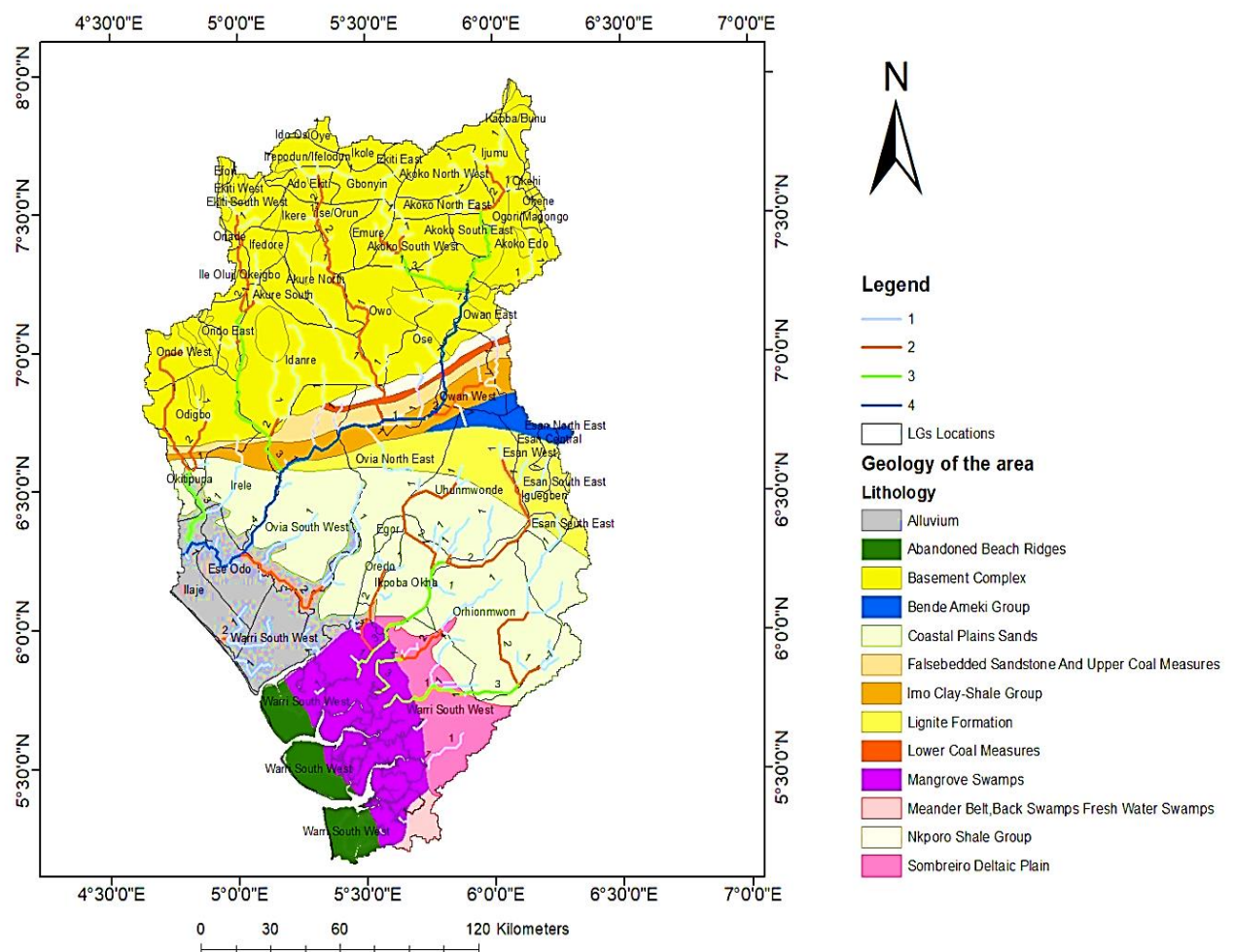


Figure 2: The geologic map of the study area.

3. Materials and Methods

3.1 Methodology

The morphology of the area was investigated by combining satellite image interpretation (Landsat TM), Digital Elevation Model and field observations. Identifying stream orders and subdivisions of the rivers based on watershed areas was the first step in this study. The orders were ranked using Rai et al. (2014) hierarchical classification system in ArcGIS. The geomorphological characteristics of the topographic and Google Terrain Image together with the Digital Elevation models were analyzed to understand the timing of the growth and the propagation of the topographic breaks. DEM data used is from Radar Topographic Missions (SRTM) downloaded from USGS site. The DEMs were used to analyze the topography and geology of the study area. Specifically, it was used to determine the uplift or subsidence of a region, and measure changes in the elevation of an area over time, which can be an indicator of tectonic activity. For example, if a region may experience an uplift, probably in reaction to the movement of a nearby structure. The prevailing drainage pattern was extracted from the DEMs, analyzed using ArcGIS and interpreted to provide information about the channel patterns and the sequences of uplift and subsidence and other pre, syn and post tectonic movement that has influenced the area. Freely available Google images were used to identify and analyse triangular facets, faceted spurs, and river meandering

The analysis of the triangular facet geometries along fault systems was investigated with the adjacent constituent segments. This approach allowed the correlation of the geometries with established patterns of a long - strike slip rate variation. The drainage density (the number of stream incision length/ basin area); hypsometric curve (ground surface distribution with altitude change). Derivatives of these indexes are described below.

The HI depicts the outline of the surface of the earth and how it changes over time and space, taking into consideration the geologic activities (surface processes) involved. It can be calculated by integrating the Hypsometric curve (HC) function (expressed in graphical form to show the elevations of certain portions of the land surface at different times Luo et al., 2018; Duan et al., 2022).

Hypsometric Integral is Mathematically expressed as:

$$Hi = \frac{M_e - Min_e}{Max_e - Min_e} \quad (1)$$

Hi = mean elevation-minimum elevation) / (maximum elevation-minimum elevation)

The Sinuosity of the Mountain Front (J):

$$J = \frac{L_{mf}}{L_s} \quad (2)$$

J = the sinuosity of the mountain front,

L_{mf} = the span of the mountain front, measured along the foot of the mountain

L_s = the straight-line length of the mountain front (Elias et.al., 2019).

Differentiated by index of ratio of valley floor width to valley depth (V_f). This parameter is calculated as:

$$V_f = \frac{2V_{fw}}{(E_{ld}-E_{sc})+(E_{rd}-E_{sc})} \quad (3)$$

where V_f is the valley floor width to valley height ratio, V_{fw} is the width of the valley floor, E_{ld} is elevations of the left valley wall, E_{rd} is elevation of the right valley wall, E_{sc} is denotes the elevation of the valley floor (e.g., Gururani et al, 2023).

SL is the stream-length index

$$SL = \frac{\Delta H}{\Delta L} * L \quad (4)$$

H is the elevation changes in a particular section, and L is the length of the channel's headwater.

Sinuosity of the Mountain fore land is described as S_{mf}

$$S_{mf} = \frac{L_{mf}}{L_s} \quad (5)$$

The distance measured around the base of the mountain front/foreland with distinct slope break is designated as L_{mf} and L_s denotes the total distance along the mountain front.

AF is the measure of the Asymmetry of a drainage basin. Calculated as:

$$AF = 100 * \left(\frac{A_r}{A_t}\right) \quad (6)$$

where A_r is the area of the right side of the drainage basin and A_t is area of the left side of the drainage basin (Baioni, 2016).

This index is a measure of

$$B_s = \frac{B_1}{B_w} \quad (7)$$

B_1 is the basin's length from the headwaters point to the subbasin's mouth, and B_w is the subbasin's width at its widest point. Elongated basins are typically associated with relatively higher tectonic activity and high B_s values. A basin with low B_s values typically has a more circular shape and indicates minor associated with low tectonism.

$$IRAT = \frac{S}{N} \quad (8)$$

where “S” is the summation of all the assigned values from the result of the landscape/geomorphic geometry used and “N” is the number of selected landscape indices (Taib et al., 2024).

Drainage density (Dd) as an index of channel spatial proximity is informed by the geology of an area, vegetation and the climate (Kim et al., 2023).

4. Results

The results of all the analyses carried out are presented below. First a total of 11 watersheds designated as subbasins were delineated, four stream orders were also identified in the basin. (Figure 3).

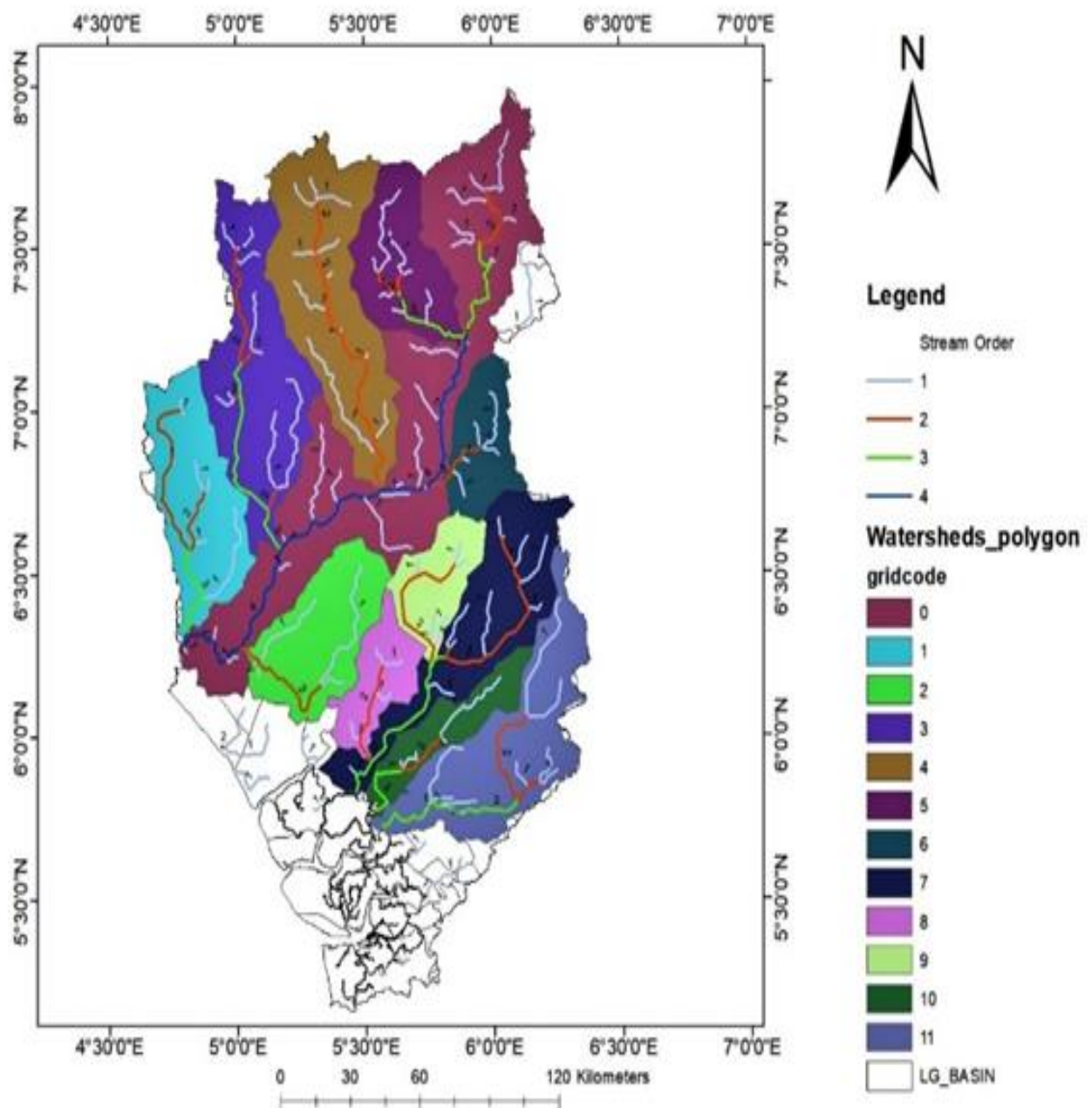


Figure 3: The Sub-basins within the area under investigation.

4.1 Stream Length Gradient (SL)

The northern part of the area under investigation forms a hilly or mountainous terrain, with appreciable slope and ephemeral drainage, the stream capability/ power is mainly a dependent on the topographic gradient (S) together with the upstream length (L) of the stream reach. It is common knowledge that any disruption in the stream gradient usually results in a rise in the SL index in the field, this increase corresponds with fault zones along all the stream profiles. These observations are traceable laterally along the strike of the exposed topographic break, it is inferred that stream profiles have been affected by tectonic reactivation along a normal fault (also as triangular facets indicating active tectonism due to fault reactivation).

The SL index was defined by Font et al. (2010) to imply the influence of stream form/morphology on stream gradient and the arrangement of stream channels in a place. The equation to determine the expression is given below.

Moussi et al. (2018) and Bermes et al. (2024) categorized SL values to gain insight into the tectonic nature as defined by SL. In this study, the SL values are also classified into three groups; Group 1 is when SL is less than 300; Group 2 is when SL is greater than 300 but less than 600; Group 3 is when SL is greater 600. The result is shown in Table 1. The major determinant of SL index is the lithology, Here, group 1 indicate an area of high tectonic activity based on our result, only sub basin 1 and the main stream at the center falls under this classification, the group 2, indicate an area of moderate tectonic activities, and according to our result sub-basins 2, 5, 7, 9, 10 and 11 falls in the region of moderate tectonic activities. Group 3 indicates an area of low tectonic activities, and based on the result; sub-basins 3, 4, 6 and 8 falls under the area of low tectonic activities.

4.2 Mountain Front Sinuosity (MFS)

Mountain Front Sinuosity (MFS) is a geomorphic index that measures the degree of tectonic activity along the front of a mountain range. MFS quantifies the extent of folding, faulting, and erosion along the mountain front, it's useful in quantifying the gradation of tectonic activity of a region. High MFS values indicate more tectonic deformation, while low MFS values indicate less deformation. Overall, MFS analysis can provide valuable information about the tectonic activity of a region, but it is just one of many methods that can be used for this purpose. Mountain front sinuosity is an index that reflects the extent of asymmetry of sinuosity along the foot of the mountain front (Bull and McFadden, 2020). According to the data from our analysis all the Sub-basins are tectonically active (Figure 4), the Smf result of areas with relatively active uplift and subsidence from 1.5 to 3, while the least modified area is between 3 to 10.

Mountain front sinuosity reveals the active nature of the mountain front to have a linear or curved outline along the topographic break/fault scarp between the northern parts (basement area) and the southern parts (sedimentary area). High sinuosity depicts a high gradient due to tectonic faulting. The sinuosity within the study area falls between 0.9 and 1.6. indicating a general tectonically active domain. The course of the rivers in the extreme north of the area under investigation can be subdivided into three sinuosity zones (Figure 4). The rivers in this area incise the mountainous basement terrains and are relatively linear with 0.09 and 1.4 sinuosity range (Figure 4). This sinuosity is relatively low upstream (Figure 4). Bedrock lithology consists of schist, granites and quartzites. Underling fault is likely responsible for the relatively linear stretch of the river channel (Giano, 2018). in the zone compared to relatively curvy channels in the southern parts (Figure 3 and Figure 4).

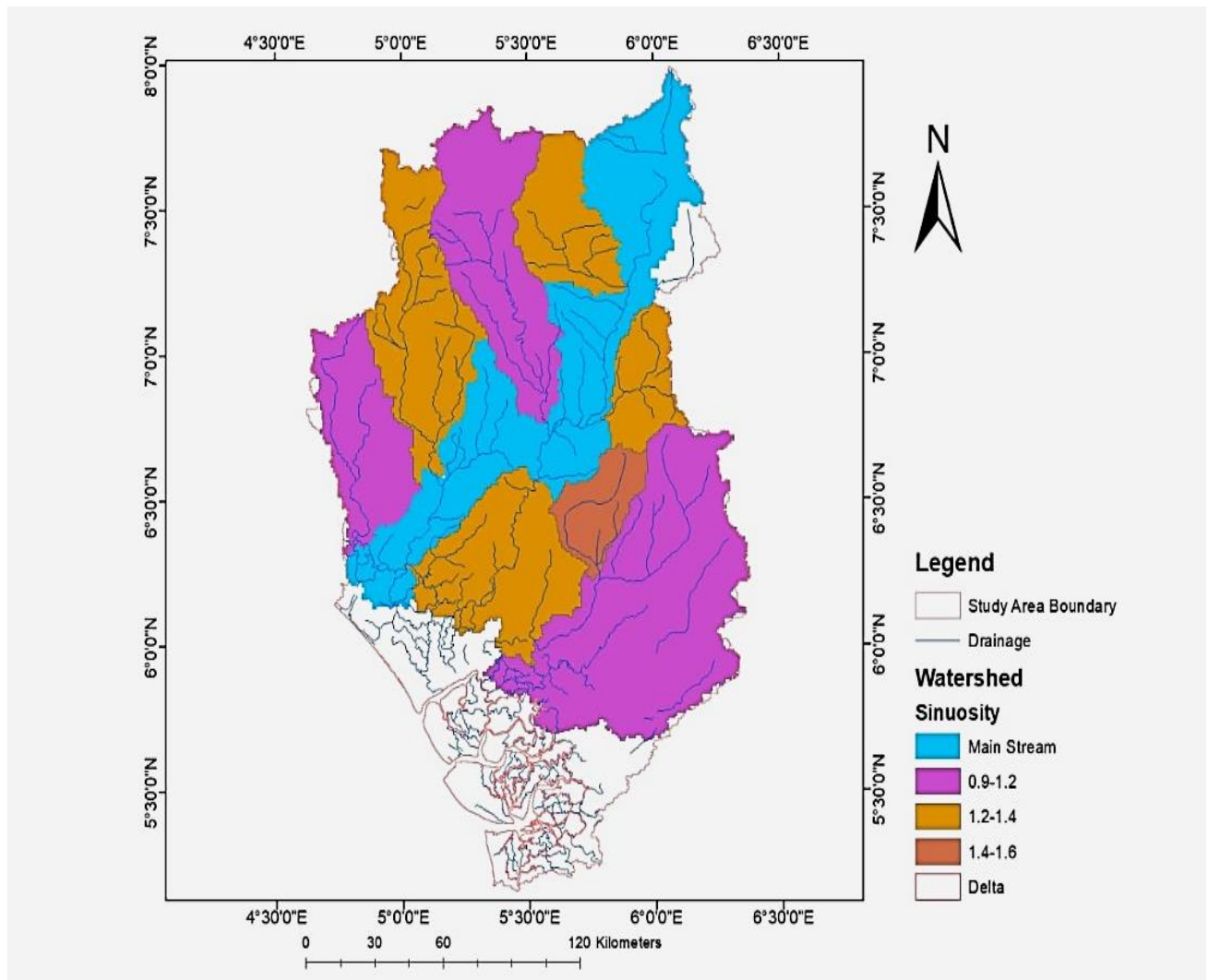


Figure 4: Final Mountain Front Sinuosity Map

4.3 Asymmetry Factor Values

The Af value in the area under investigation varies from 44.31 to 81.51 (Figure 5). The analysis revealed that Sub-Basin 4 and 8 belong to Class I where the Sub-basin tilted right toward its main trunk; Sub-Basin 6 and 7 belong to Class II, where we have little or no tilting of the Sub-basin and Sub-Basin 1, 2, 3, 5, 9, 10, and 11 (see Figure 3) belongs to Class III, with a left tilt to its main trunk. It was also noted that watersheds 1 and 4 had the maximum and minimal values of basin asymmetry, respectively (Table 1).

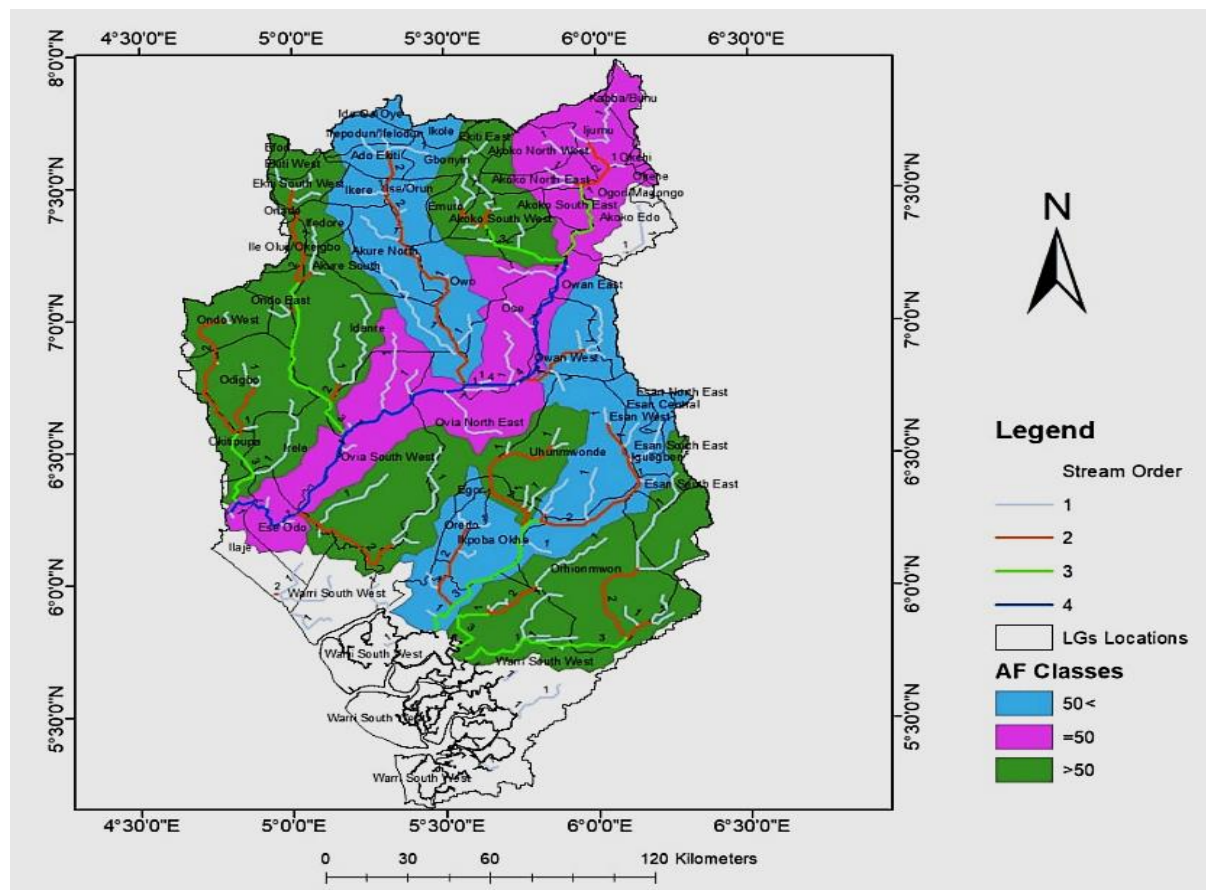


Figure 5: Asymmetry Factor value map showing the categories.

4.4 Hypsometry curves

Hypsometry integral analysis is a method used to assess the distribution of elevation in a region. It involves calculating the area of land at each elevation above sea level and plotting this as a cumulative distribution curve. Changes in the shape of the hypsometry curve can indicate tectonic uplift or subsidence. For example, if a region experiences uplift, the hypsometry curve will shift towards higher elevations, indicating an increase in the area of land at higher elevations. Similarly, subsidence will cause the hypsometry curve to shift towards lower elevations.

The hypsographic index approximates the elevation of basins, to determine the volume of sediments and the erosion that affected the basin (Poyraz et. al., 2011). Munipour and Najad (2011) gave the equation that relates to the expressions.

$$Hi = (\text{minimum elevation} - \text{average elevation}) / (\text{maximum elevation} - \text{minimum elevation}).$$

In that the value of this index is influenced by rock strength in addition to other factors, it is comparable to the SL index (Della-Seta et.al., 2017). In general, high HI values indicate that fewer uplands have been eroded, suggesting a younger and tectonically mobile landscape. Each sub-basin's HI was calculated using Arcmap. The Table 2 shows that it varies from 0.24 in subbasin 9 to 0.46 in subbasins 5. The following three classes of HI values were identified in relation to the curve's shape: class 1 with hypsometric curves that are convex (0.51-0.78) none of the sub-basins in this study fall within this class; class 2 with concave-convex hypsometric curves ranging from (0.37 to 0.50). Sub-basins 5, 6 and 10 fall within this class. Class 3 with concave hypsometric curves ranging from 0- 0.37, sub-basins 1,2,3,4,7,8,9, and 11 fall within

this class and can be interpreted as areas where fluvial activities have reached the mature and old stages of development respectively (Figure 6).

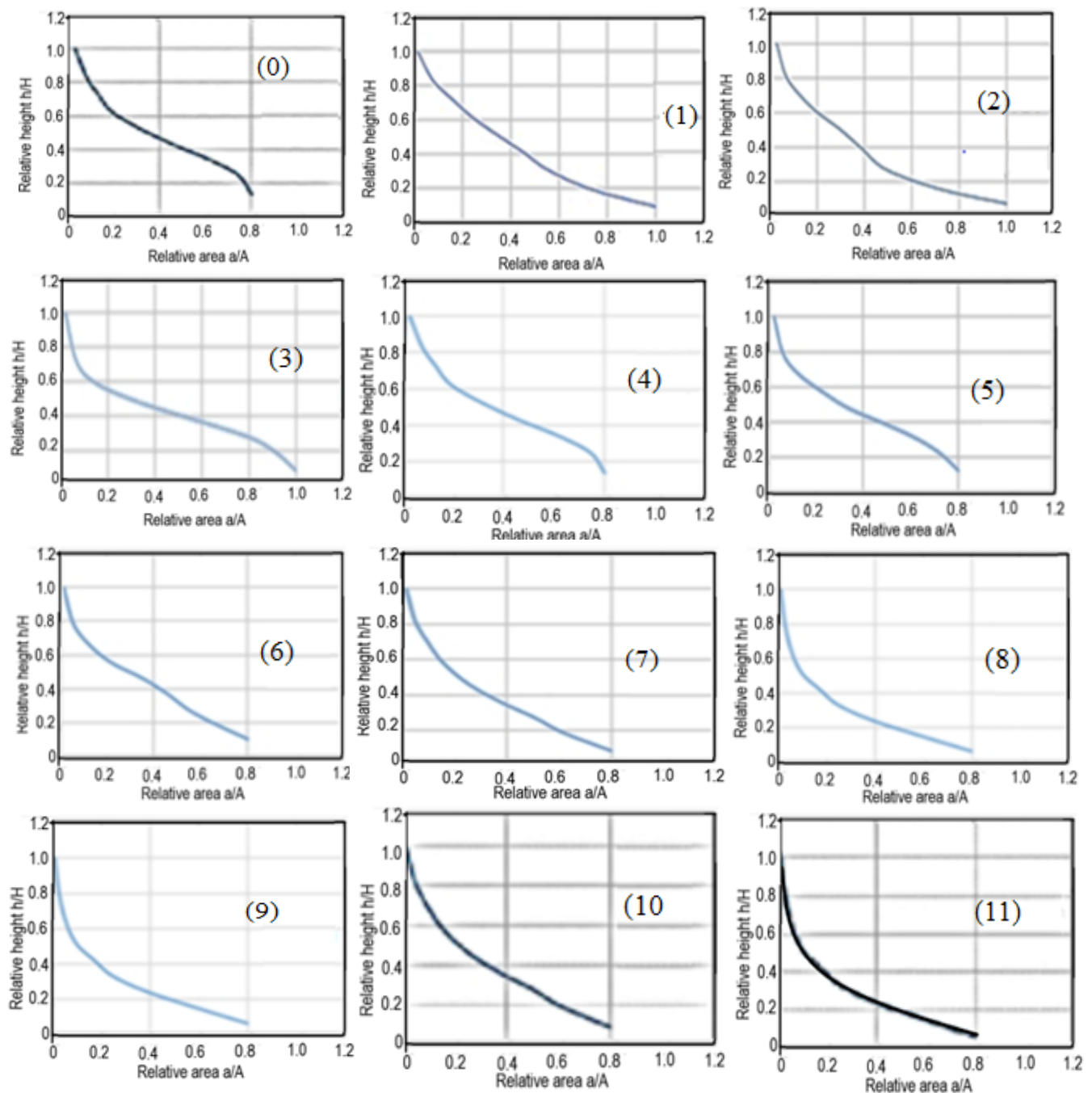


Figure 6: Hypsometry curves, Label represent the basin number.

4.5 Basin Shape Index (BS)

Changes in the basin shape index can indicate changes in tectonic processes such as folding and faulting, subsidence and uplifts (Chen and Willett, 2016). For example, basin elongation

can be caused by extensional tectonics, while basin contraction may be caused by compressional tectonics.

Bl is the land area extent of a basin from where the river or stream emanates to the outlet. Bw is the widest width of the basin. Stretched basin will have high Bs indicating that the basin is tectonically altered. Basins with low Bs are more circular in shape and this means they have not been significantly altered by tectonic forces. The calculated Bs for each of the 11 subbasins can be classified into three classes (Figure 7): class 1 (2.80-4.0 and above) i.e. Sub basin 1,3,4,7,8,10 and 11 their class are considered High in tectonic activities; class 2 (1.50-2.79) i.e. Sub-basin 2,5,6, and 9 are moderately tectonic and class 3 (1.20-1.50) i.e. low tectonic does not exist within the study area.

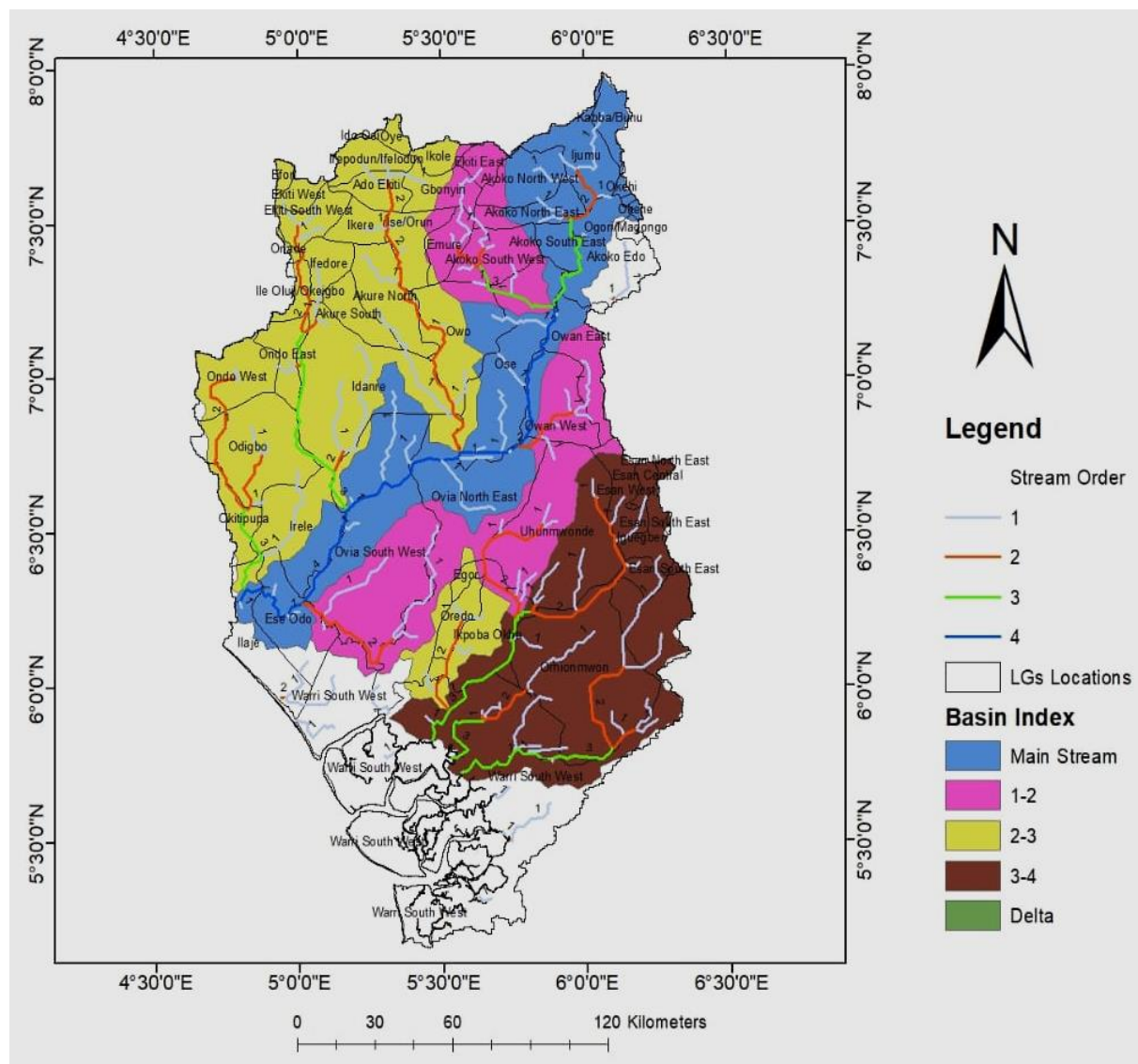


Figure 7: Final Basin Shape Index Map

Table 1: Result of geomorphic indexes for each of the sub-basins

SB	SL	(AF)	(HI)	(BS)	(J)	(IRAT)
SB1	620	81.506822	0.28106543	2.13447783	1.3221869	105.05
SB 2	400	59.847943	0.31712122	1.422209	1.1280152	68.54
SB 3	250	73.399391	0.28979743	2.46713169	1.16226974	51.46
SB 4	250	44.305497	0.34111923	2.82456687	1.24532217	45.74
SB 5	310	56.676026	0.46213557	1.71880721	1.12332089	55.1
SB 6	180	48.944047	0.37101055	1.54527749	1.10343112	36.39
SB 7	390	49.839047	0.34684758	3.77058093	1.24219	67.04
SB 8	260	46.090001	0.29694335	2.04291175	1.18990015	47.92
SB 9	350	60.11881	0.24778939	1.53870708	1.52045177	62.69
SB 10	550	52.259708	0.4133669	4.89363683	1.26464563	89.76
SB 11	400	55.66985	0.31517939	3.73022661	1.24322406	70.19

KEY

SSB - SUB-BASIN

SL - SLOPE GRADIENT

AF - ASSYMETRIC FACTOR

HI - HYPSONETRIC INTEGRAL

BS - BASIN SHAPE INDEX

J - MOUNTAIN FRONT SINOUSITY

IRAT - INDEX RELATIVE ACTIVE TECTONIC

4.6 Index Relative Active Tectonic (IRAT)

IRAT explains the morphological parameters that are relevant to attribute relative active tectonics to a spatial zone (Ali and Ikbali, 2020; Kumar et al., 2022). This index helps in identifying basin areas that has been deformed by tectonics. Some of the imprint of deformation by tectonism are stream deflections, abrupt change in gradient (due to uplift or subsidence), formation of waterfalls, meandering, deep valleys etc. The average of the calculated geomorphic index is presented in Table 2. Minimum of two indices is required to quantify the relative tectonic activity in active mountain ranges (Quye-Sawyer et al., 2021). “IRAT” = $(AF + Mfs + BS + HI + SL) / 5$. The “IRAT” indices are categorized into four, with each describing the extent of comparative tectonic activity, Category 1 is (1.0 to 1.5), category 2 (1.5 to 2), category 3 (2.1 to 2.5), and category 4 (>2.5) with very high, high, moderate, and low relative tectonic activity, respectively (Othman and Omar, 2023). The result from this study indicates that the tectonic activities in this Benin Basin can be classified as high with just three of the basins showing moderate tectonic activity while the remaining sub-basins show moderately high tectonic activity.

Table 2. “IRAT” value and category of sub-basins in Benin-Owena Basin

Sub-basins	AF	Mfs (J)	BS	HI	SL	IRAT	IRAT Category
1	3	1	1	3	1	1.8	2
2	3	1	2	3	2	2.2	3
3	3	1	1	3	3	2.2	3
4	1	1	1	3	3	1.8	2
5	3	1	2	2	2	2.0	2
6	2	1	2	2	3	2.0	2
7	2	1	1	3	2	1.8	2
8	1	1	1	3	3	1.8	2
9	3	1	2	3	2	2.2	3
10	3	1	1	2	2	1.8	2
11	3	1	1	3	2	2.0	2

This index indicates rupture of the topography which can be related to tectonic effect, type of bedrock and amount of rainfall.

4.7 Triangular Facets and River Meandering

Facets are major topographic features built overactive normal faults, and they are widespread in diverse extensional settings. They represent one of the most prominent geomorphic features on active normal fault scarps (Tesson et al., 2021). This feature is initiated when the hanging wall of a normal fault descends to form a topographic step/scarp. Followed by the continuous incision of the block above the hanging wall by drainage (Barnes and Barraud, 2012; Azañón et al., 2015; Chen and Willett, 2016). A combination of both tectonic and drainage forces is responsible for the formation of facets, while the geometry of the facets depends on the rock strength and ability to resist erosion. Triangular facet development integrates increasing displacement over the entire growth period of a normal fault and can be used to determine the evolution of normal faults (Tesson et al., 2021).

The faceted spurs close to the east are already in a steady state, the drainage divide is linear and largely parallel to one another, especially (Figure 8a and 8b). The coalition of the river divides of the last two faceted spurs (close to River Niger), branch together to form new strike-perpendicular spurcrests, the facets have smooth scalp without pronounced incisions. While the other facet spurs to the west (Figure 8a and 8b) form facet imbricates due to incomplete merging of former divides and divergence of divides. Lack of pronounced incisions can be attributed to low precipitation rate or erodibility of the rock. Easily erodible rocks will have more incisions (Chebotarev et al., 2021).

Facet imbrication appears more on the facets at the western parts because of incomplete coalescence of smaller divides (Figure 9a and b). The facets on the eastern side, close to River Niger are in steady state because the number of catchment 8 is constant, the crest heights and valley depths are stable implying a progressive maturity from the west to the east.

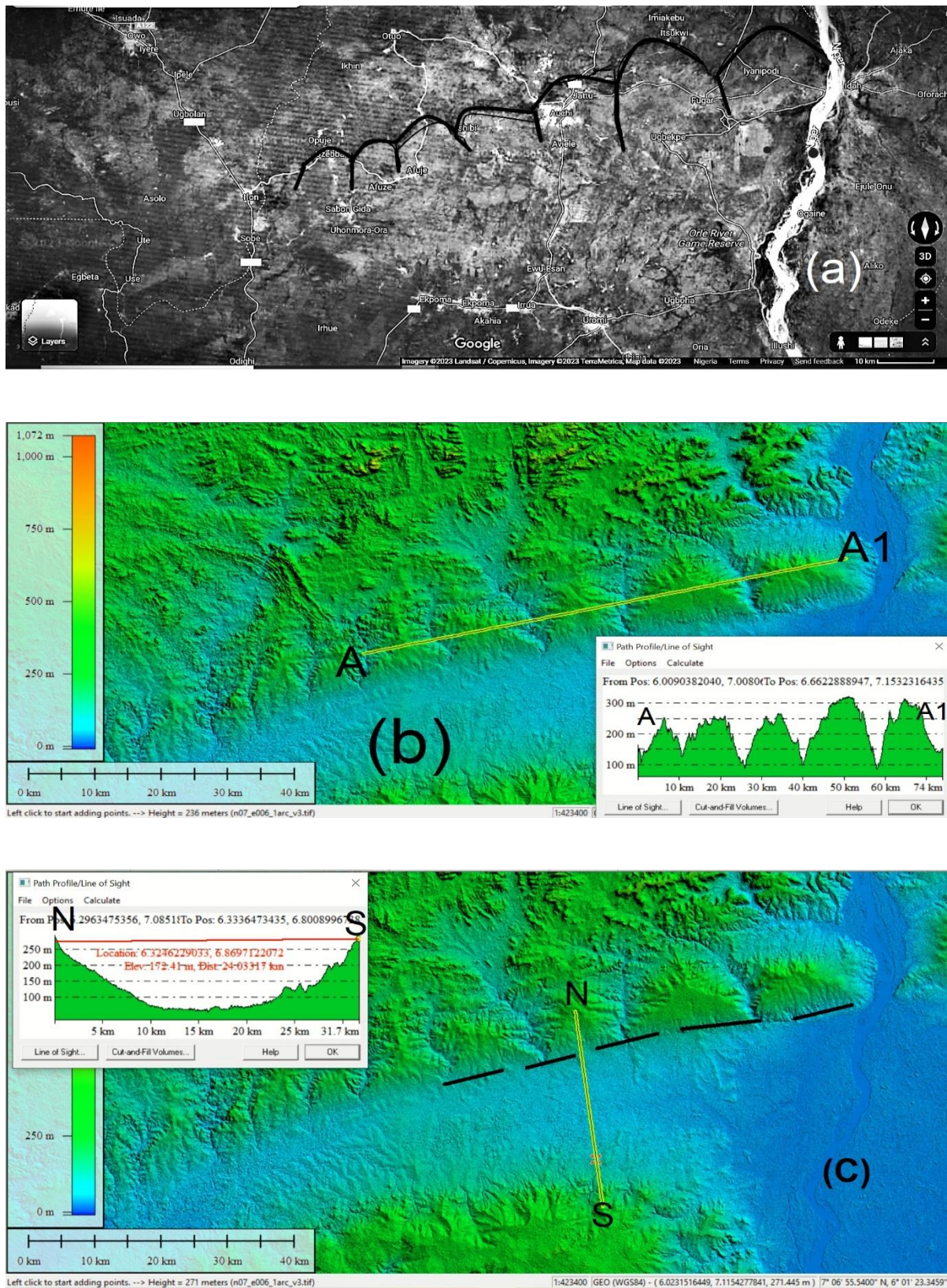


Figure 8: (a) Google map of study area showing the triangular facets marked in black west of River Benue. (b) shows the Triangular facets along strike variation in geometry that can be linked to the process of fault evolution. (c) demonstrates normal fault throw and slope of triangular facets.

4.7.1 Length and Height of facets

The gradient of water increases along the normal fault (facets), down stepping from North to south (Figure 8c). Facets with anomalously high facet height to width ratios (Figure 8b) are more likely located along the fault segments, Fault segment locations show a preference towards larger facet and less incised geometries. From west to east, the facets show progressive maturity. The dip direction of the normal fault results in the uplifting of the riverbed/footwall to form the horst and the subsiding of the central part/hanging wall of the fault to form a half graben (Figure 8c). The fault is extending southwards towards (S).

4.7.2 River Meandering

Modification of stream channels along an obstruction may lead to a single channel forming an anastomosing system of channels around the obstruction resulting in river meandering (Basnayaka et al., 2022). Meandering might indicate a lateral tilt, incised meandering, change in river flow direction along the valley floor plain. Increasing meandering reduces slope, while cut-offs increase slope (Semwal and Chauniyal, 2022). Reduced gradient along the valley will result in the formation of lakes, thus indicating the first stage of stream disruption. The lakes are likely to develop fully around River Orle (i.e. around Orle River) and around latitude $6^{\circ} 13'50''$ in Figure 9. There is a strong likelihood that the meandering is related to deformation. The floor of the down warped portion of the area under investigation consist of the different categories of meandering- the straight segment channel indicating active and recent tectonics Figure 9, which are found along the line of fault due to the presence of linear zone of weakness underneath it. Straight channels allow increase in water velocity, better water flow and might reduce the risk of flooding due to easy removal of backlogs along the channel. The floor of the downwarped portion of the area under investigation consist of the different categories of meandering- the straight segment channel indicating active and recent tectonics, are found along the line of fault due to the presence of linear zone of weakness underneath by a fault line.

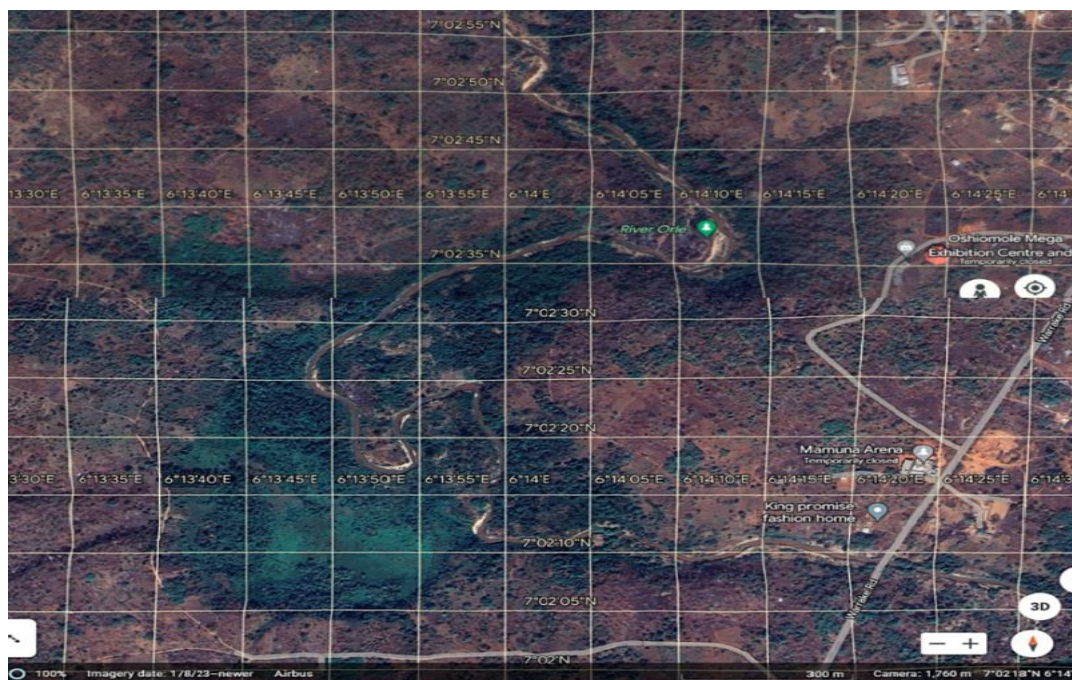


Figure 9: Google image of study area showing lake formation around River Orle and meandering streams

5. Discussion

River drainages respond to subtle tectonic changes by tilting or changing the slope of alluvial river profiles. It is commonly assumed that drainage areas are the same to the left and right of the trunk river. However, regional-scale dipping of more resistant rock layers, tectonic tilting or the presence of strike-slip fault zones (or a combination of these factors) may cause rivers to alter laterally. Downstream/downslope tilt along the valley area increases stream sinuosity, and growth of meanders maintain a constant gradient. While the upstream end of an uplift will have a reduced sinuosity, this is caused by a decrease in the gradient of the valley floor (Bufe et al., 2016; Wang et al., 2024). Channel sinuosity increased in response to the steepened valley floor (Turowski, 2018) on the downstream side of the uplift axis (Figure 8b) or the upstream side of the subsidence (Figure 9c) respectively. The meandering might also indicate a lateral tilt and deformation of the valley floor plain. Increasing meandering reduces slope, while cut-offs increase slope. A reduced gradient along the valley will result in the formation of lakes, thus indicating the first stage of stream disruption. The lakes are likely to develop fully around the River Orle (Figure 9 i.e. around Orle River) and latitude $6^{\circ} 13'50''$ in Figure 10. indicating more flow with decreased water velocity. The floor of the down warped portion of the area under investigation consists of the different categories of meandering (the straight segment channel indicating active and recent tectonics) in Figure 9, which are found along the line of fault due to the presence of a linear zone of weakness underneath it. Straight channels allow an increase in water velocity, better water flow and might reduce the risk of flooding due to easy removal of backlogs along the channel. Channel sinuosity is also influenced by lithological changes, this becomes more obvious when different lithologies are brought together by faulting. The floor of the down warped portion indicates down warping (subsidence/concave) while the uplifted areas are convex (Figure 9).

The counter-reaction of rivers shows deep parallel incisions of the basement outcrops and strong erosion of the sedimentary basin as evidenced by the wide valley width and deposition of more sediment load (Dahomey Basin). The rivers are dynamic, possessing more erosive powers at their youthful stage, located close to mountainous headwater areas, and progressing to mature and old-age stream developmental stages around the sedimentary basins.

The subsidence that led to the formation of this basin must have been accompanied by a period of tensional stress and normal faulting with the lowering of the hanging walls (Figure 7). Few periods of uplift and more periods of subsidence were documented. This conforms with the study conducted by (Salami and Olorunfemi, 2014; Akande et al., 2011; Opara, 2011) who concluded that the basin has experienced a complex history of tectonic activity, including multiple phases of faulting and uplift with buried faults that are not visible at the surface. The study revealed that the basin has experienced significant tectonic activity, including faulting, subsidence and uplift. It is noteworthy that the faults in the region are aligned with major regional tectonic trends, confirming previous and ongoing tectonic activities in the region.

Within the study area, 11 watersheds or subbasins were delineated, characterized by four stream orders. Analysis of river courses revealed distinct sinuosity zones, with the northern region exhibiting relatively straight rivers due to the underlying bedrock lithology. The sinuosity increases southward and this can be attributed to changes in the lithology and valley morphology. Neotectonic activities are evidenced by topographic variations and steep valley walls. The Af values within the study area indicate variations in basin asymmetry, suggesting different degrees of tilting and tectonic activity. The hypsometry curve provides insights into elevation changes, reflecting tectonic and subsidence processes and areas that are susceptible to erosion. Most of the subbasins are predominantly in an early to late stage of a maturity stage.

Meandering and channel sinuosity increase downstream due to steepened valley floors, while uplifted areas exhibit convexity and subsided areas show concavity. However, the recent climate change with a significant increase in precipitation might lead to more downcutting and channel deepening of rivers at this stage. As streams mature, they tend to exhibit flooding and meandering (Scorpio and Comiti, 2024), highlighting the importance of thorough preparation to mitigate flooding caused by rising precipitation due to climate change.

Basin asymmetry serves as an indicator of active tectonics, with subbasins classified into high, moderate, and low tectonic activity classes. Results suggest high tectonic activity within the region, with triangular facets indicating extensional settings and fault activity. Triangular facet morphological attributes have helped in retrieving long-term slip rate information (Turker et al., 2020) and future zones of extension of the faults this area. This information will assist in locating area for the installation of GPS (Global Positioning System), for earthquake monitoring and possible mitigation of seismic hazards (Pirrotta et al., 2021). Further analysis reveals how river drainages respond to tectonic changes, altering laterally due to factors like regional rock layer dipping, tectonic tilting, or strike-slip fault zones. The study suggests that the formation of the basin was accompanied by periods of tensional stress, normal faulting, and subsidence, aligning with previous research and indicating possible ongoing tectonic activities in the region. The southern parts reveal evidence of previous subsidence and sedimentary infilling.

6. Conclusions

This research explores the evaluation of geomorphic parameters as a pilot study to determine the relative tectonic state of the Owena-Bening basin within the eastern parts of the Dahomey Basin. The study reveals that the basin has experienced differential uplift and erosion rates from time to time in the geological past. This is corroborated by the morphometric and morphotectonic analysis results which have proved useful in identifying drainage basins that could be prone to hydrogeomorphic hazards. Basin depth is deepest over downfaulted or downfolded areas, and thinnest over areas of uplift. The study evaluates the relationships between triangular facet geometry (i.e., area, height and slope) and fault slip; and explains how tectonic interactions of faults produce variations in triangular facet geometry along fault systems of segments. The triangular facet geometry is a basis for identifying pre-linkage fault segment boundaries along active normal faults, which may have been obscured during the fault-linking process. The investigation has also helped categorize the area into high, moderate and low tectonically active areas. The result has implications for locating monitoring equipment for earthquake activities (Mahmood and Gloaguen, 2012). In conclusion, the study provides a comprehensive understanding of tectonic influences on drainage systems and river behavior. It highlights the importance of considering geological structures and lithological changes in interpreting landscape evolution and tectonic activity within the studied basin.

References

- Akande, S.O., Ojo, O.J., Adeleye, O.A., Egenhoff, S.O., Obaje, N.G., Erdtmann, B.D. (2011): Stratigraphic Evolution and Petroleum Potential of Middle Cretaceous Sediments in the Lower and Middle Benue Trough, Nigeria: Insights from New Source Rock Facies Evaluation. *Petroleum Technology Development Journal* ISSN 1595-9104 v11.

- Ali, S.A. and Ikbali, J. (2020): Assessment of relative active tectonics in parts of Aravalli mountain range, India: implication of geomorphic indices, remote sensing, and GIS. *Arabian Journal of Geosciences*, 13, pp.1-16. <https://doi.org/10.1007/s12517-019-5028-2>
- Ambili V, Narayana AC (2014): Tectonic effects on the longitudinal profiles of the Chaliyar River and its tributaries, southwest India. *Geomorphology*, 217, 37–47. <https://doi.org/10.1016/j.geomorph.2014.04.013>
- Anand AK, Pradhan SP (2019): Assessment of active tectonics from geomorphic indices and morphometric parameters in part of Ganga basin. *Journal of Mountain Science*, 16(8), pp.1943-1961. <https://doi.org/10.1007/s11629-018-5172-2>
- Azañón, J.M., Galve, J.P., Pérez-Peña, J.V., Giaconia, F., Carvajal, R., Booth-Rea, G., Jabaloy, A., Vázquez, M., Azor, A. and Roldán, F.J. (2015): Relief and drainage evolution during the exhumation of the Sierra Nevada (SE Spain): Is denudation keeping pace with uplift?. *Tectonophysics*, 663, pp.19-32. <https://doi.org/10.1016/j.tecto.2015.06.015>
- Baioni, D. (2016): Analysis of Drainage Basin Asymmetry in the Ventena River, Northern Apennines (Central Italy). *International Journal of Earth & Environmental Sciences*, 1(121), pp.1-5. [10.15344/2456-351X/2016/121](https://doi.org/10.15344/2456-351X/2016/121)
- Barnes, G. and Barraud, J. (2012): Imaging geologic surfaces by inverting gravity gradient data with depth horizons. *GEOPHYSICS*, 77(1), G1–G11. doi:10.1190/geo2011-0149.1. <https://doi.org/10.1190/geo2011-0149.1>
- Baruah, M. P., Bezbaruah, D., and Goswami, T. K. (2020): Active tectonics deduced from geomorphic indices and its implication on economic development of water resources in South-Eastern part of Mikir massif, Assam, India. *Geology, Ecology, and Landscapes*, 6(2), 99–112. <https://doi.org/10.1080/24749508.2020.1754705>
- Bermes, A., Tomeniuk, O. and Bogucki, A. (2024): Stream Length-Gradient (SL) Index of the Kremenets Mountains as One of the Indicators of Modern Tectonic Movements of the Region. In *International Conference of Young Professionals «GeoTerrace-2024»* (Vol. 2024, No. 1, pp. 1-5). European Association of Geoscientists & Engineers. <https://doi.org/10.3997/2214-4609.2024510004>
- Basnayaka, V., Samarasinghe, J.T., Gunathilake, M.B., Muttill, N., Hettiarachchi, D.C., Abeynayaka, A. and Rathnayake, U. (2022): Analysis of meandering river morphodynamics using satellite remote sensing data—an application in the lower Deduru Oya (River), Sri Lanka. *Land*, 11(7), p.1091.
- Bufe, A., Paola, C. and Burbank, D.W. (2016): Fluvial bevelling of topography controlled by lateral channel mobility and uplift rate. *Nature Geoscience*, 9(9), pp.706-710. <https://doi.org/10.1038/ngeo2773>

- Bull, W.B. and McFadden, L.D. (2020): Tectonic geomorphology north and south of the Garlock fault, California. In *Geomorphology in arid regions* (pp. 115-138). Routledge.
- Chebotaiev, A., Arzhannikova, A. and Arzhannikov, S. (2021): Long-term throw rates and landscape response to tectonic activity of the Tunka Fault (Baikal Rift) based on morphometry. *Tectonophysics*, 810, p.228864. doi: [org/10.1016/j.tecto.2021.228864](https://doi.org/10.1016/j.tecto.2021.228864)
- Chen, C.Y. and Willett, S.D. (2016): Graphical methods of river profile analysis to unravel drainage area change, uplift and erodibility contrasts in the Central Range of Taiwan. *Earth Surface Processes and Landforms*, 41(15), pp.2223-2238. doi:[10.1002/esp.3986](https://doi.org/10.1002/esp.3986)
- Della Seta, M., Esposito, C., Marmoni, G.M., Martino, S., Mugnozza, G.S. and Troiani, F., (2017). Morpho-structural evolution of the valley-slope systems and related implications on slope-scale gravitational processes: New results from the Mt. Genzana case history (Central Apennines, Italy). *Geomorphology*, 289, pp.60-77. DOI: [10.1016/j.geomorph.2016.07.003](https://doi.org/10.1016/j.geomorph.2016.07.003)
- Duan, Y., Pei, X. and Zhang, X. (2022): The Hypsometric Integral Based on Digital Elevation Model for the Area West of Lvliang Mountains in Loess Plateau, Shanxi, China. *Frontiers in Earth Science*, 10, p.827836. DOI: [10.3389/feart.2022.827836](https://doi.org/10.3389/feart.2022.827836)
- Elias, Z., Sissakian, V.K. and Al-Ansari, N. (2019): Assessment of the Tectonic Activity in Northwestern Part of the Zagros Mountains, Northeastern Iraq by Using Geomorphic Indices. *Geotech Geol Eng* 37, 3995–4007. <https://doi.org/10.1007/s10706-019-00888-z>
- Ezati, M. and Gholami, E., (2022) Neotectonics of the Central Kopeh Dagh drainage basins, NE Iran. *Arabian Journal of Geosciences*, 15(10), p.992. <https://doi.org/10.1007/s12517-022-10280-6>
- Fillon, C., Huismans, R.S. and van der Beek, P. (2013): Syntectonic sedimentation effects on the growth of fold-and-thrust belts. *Geology*, 41(1), 83–86. <https://doi.org/10.1130/G33531.1>
- Font, M., Amorese, D. and Lagarde, J.L. (2010): DEM and GIS analysis of the stream gradient index to evaluate effects of tectonics: the Normandy intraplate area (NW France). *Geomorphology*, 119(3-4), pp.172-180. <https://doi.org/10.1016/j.geomorph.2010.03.017>
- Fryirs, K.A. and Brierley, G.J. (2012): Geomorphic analysis of river systems: an approach to reading the landscape. John Wiley & Sons.
- Giano, S.I, Pescatore, E, Agosta, F. and Prosser, G. (2018): Geomorphic evidence of Quaternary tectonics within an underlap fault zone of southern Apennines, Italy. *Geomorphology*, 303,172–190. <https://doi.org/10.1016/j.geomorph.2017.11.020>
- Gugliotta, M. and Saito, Y. (2019): Matching trends in channel width, sinuosity, and depth along the fluvial to marine transition zone of tide-dominated river deltas: The need for

a revision of depositional and hydraulic models. *Earth-Science Reviews*.

<https://doi.org/10.1016/j.earscirev.2019.02.002>

- Gururani, K., Kotlia, B.S., Chand, P., Kukreti, M., Parashar, D., Kalkhundiya, A., Bhatt, P.K. and Pandey, A. 2023: Morphometric Analysis of Tectonically Active Bhimtal-Naukuchiatal Lake Basin, Kumaun Himalaya. *Current World Environment*, 18(2), p.855. DOI: [10.12944/CWE.18.2.32](https://doi.org/10.12944/CWE.18.2.32)
- Kim, S., Yoon, S.K. and Choi, N. (2023) Evaluating the Drainage Density Characteristics on Climate and Drainage Area Using LiDAR Data. *Applied Sciences*, 13(2), p.700. <https://doi.org/10.3390/app13020700>
- Koroknai, B., Wórum, G., Tóth, T., Koroknai, Z., Fekete-Németh, V. and Kovács, G., 2020: Geological deformations in the Pannonian Basin during the neotectonic phase: New insights from the latest regional mapping in Hungary. *Earth-Science Reviews*, 211, p.103411. <https://doi.org/10.1016/j.earscirev.2020.103411>
- Kumar, N., Dumka, R.K., Mohan, K. and Chopra, S. (2022): Relative active tectonics evaluation using geomorphic and drainage indices, in Dadra and Nagar Haveli, western India. *Geodesy and Geodynamics*, 13(3), pp.219-229. <https://doi.org/10.1016/j.geog.2022.01.001>
- Luo, M., Xu, Y., Mu, K., Wang, R. and Pu, Y. (2018): Spatial variation of the hypsometric integral and the implications for local base levels in the Yanhe River, China. *Arabian Journal of Geosciences*, 11, pp.1-9. <https://doi.org/10.1007/s12517-018-3711-3>
- NiMet, (2023): Nigerian Meteorological Agency (Nimet) Predicts Early Onset Of Rainfall, Severe Dry Spell In Northern, Central States. <https://nimet.gov.ng/scp/>
- Mahmood, S.A. and Gloaguen, R. (2012): Appraisal of active tectonics in Hindu Kush: Insights from DEM derived geomorphic indices and drainage analysis, *Geoscience Frontiers* 3 (4) 407-428pp. doi:10.1016/j.gsf.2011.12.002.
- Misra, A., Agarwal, K., Kothyari, G., Talukdar, R. and Joshi, G. (2020): Quantitative Geomorphic Approach for Identifying Active Deformation in the Foreland Region of Central Indo-Nepal Himalaya. *Geotectonics*. 54. 543-562.doi: 10.1134/S0016852120040093.
- Moussi, A., Rebaï, N., Chaieb, A., and Saâdi, A. (2018): GIS-based analysis of the Stream Length-Gradient Index for evaluating effects of active tectonics: a case study of Enfidha (North-East of Tunisia). *Arabian Journal of Geosciences*, 11(6). doi:10.1007/s12517-018-3466-x
- Munipour, M. and Najad, H.T. (2011): Tectonic Geomorphology setting of Khayiz anticline derived from GIS processing, Zagros Mountain, Iran. *Asian Journal of Earth Sciences* 4-3, 171-182. <https://scialert.net/abstract/?doi=ajes.2011.171.182>

- Othman, A.T., Omar, A.A. (2023): Evaluation of relative active tectonics by using geomorphic indices of the Bamo anticline, Zagros Fold-Thrust Belt, Kurdistan Region of Iraq, *Heliyon*, Volume 9, Issue 7, e17970, ISSN 2405-8440.
<https://doi.org/10.1016/j.heliyon.2023.e17970>
- Okpoli, C.C and Eyitoyo, F.B. (2016): Aeromagnetic study of Okitipupa region, Southwestern Nigeria. *International Basic and Applied Research Journal*, volume 2, issue no. 7, pp. 1-20.
- Opara, A.I. (2011): Estimation of the Depth to Magnetic Basement in Part of the Dahomey Basin, Southwestern Nigeria. *Australian Journal of Basic and Applied Sciences*. 5(9): 335-343.
- Opara, A., Ekwe, A., Okereke, C, Oha, I.A. and Nosiri O. (2012): Integrating Airborne Magnetic and Landsat Data for Geologic Interpretation over part of the Benin Basin, Nigeria. *Pacific Journal of Science and Technology*. 13. 556-571.
- Olabode, S.O. (2015): Subsidence Patterns in The Nigerian Sector Of Benin (Dahomey) Basin: Evidence From Three Offshore Wells. *Ife Journal of Science* vol. 17, no. 2.
<https://www.ajol.info/index.php/ijss/article/view/131784>.
- Oladele, S., and Ayolabi, E.A. (2014): Geopotential imaging of the Benin basin for hydrocarbon prospectivity. *NAPE Bull*. 26(1):101–112.
- Pant, N., Dubey, R.K. and Bhatt, A. (2020): Soil erosion and flood hazard zonation using morphometric and morphotectonic parameters in Upper Alaknanda River basin. *Nat Hazards* 103, 3263–3301. <https://doi.org/10.1007/s11069-020-04129-y>.
- Pirrotta, C., Barberi, G., Barreca, G., Brighenti, F., Carnemolla, F., De Guidi, G., Monaco, C., Pepe, F. and Scarfi, L. (2021): Recent activity and kinematics of the bounding faults of the Catanzaro trough (Central Calabria, Italy): New morphotectonic, geodetic and seismological data. *Geosciences*, 11(10), p.405.
<https://doi.org/10.3390/geosciences11100405>
- Poyraz., M., Taskın., S. and Keles, K. (2011): Morphometric approach to geomorphologic characteristics of Zeytinli Stream basin. *Procedia-Social and Behavioral Sciences*, 19, pp.322-330. <https://doi.org/10.1016/j.sbspro.2011.05.138>
- Quye-Sawyer, J., Whittaker, A.C., Roberts, G.G. and Rood, D.H. (2021): Fault throw and regional uplift histories from drainage analysis: Evolution of southern Italy. *Tectonics*, 40(4), p.e2020TC006076. <https://doi.org/10.1029/2020TC006076>
- Radaideh, O.M. and Mosar, J. (2019): Tectonics controls on fluvial landscapes and drainage development in the westernmost part of Switzerland: Insights from DEM-derived geomorphic indices. *Tectonophysics*, 768, p.228179.

- Rai, P.K, Mishra, S., Ahmad, A., Mohan, K. (2014): A GIS-based Approach in Drainage Morphometric Analysis of Kanhar River Basin, India, *Applied Water Science*. DOI 10.1007/s13201-014-0238-y.
- Salami, B.M. and Olorunfemi, M.O. (2014): Hydrogeophysical evaluation of the groundwater potential of the central part of Ogun State, Nigeria. *Ife Journal of Science* vol. 16, no. 2. 291-299.
- Scorpio, V. and Comiti, F. (2024): Channel changes during and after extreme floods in two catchments of the Northern Apennines (Italy), *Geomorphology*, Volume 463, 109355, ISSN 0169-555X, <https://doi.org/10.1016/j.geomorph.2024.109355>.
- Semwal, S. and Chauniyal, D.D. (2022): Tectonic Control on the Meanders Pattern of Alaknanda River in Srinagar Valley, Garhwal Himalaya, India. In: Bhattacharya, H.N., Bhattacharya, S., Das, B.C., Islam, A. (eds) *Himalayan Neotectonics and Channel Evolution*. Society of Earth Scientists Series. Springer, Cham. https://doi.org/10.1007/978-3-030-95435-2_5.
- Sharma, M.P. and Kujur, A. (2012): Application of Remote Sensing and GIS for groundwater recharge zone in and around Gola Block, Ramgargh district, Jharkhand, India. *Int J Sci Res Publ* 2(2):1–6.
- Singh, R., Shekhar, M., Pandey, V.K., Kumar, R. and Sharma, R.K. (2018): Causes, and geomorphological effects of large debris flows in the lower valley areas of the Meru and Gangotri glaciers, Bhagirathi basin, Garhwal Himalaya (India). *Remote Sensing Lett* 9 (8):809–818. <https://doi.org/10.1080/2150704X.2018.1484956>
- Shit, P.K., Bera, B., Islam, A., Ghosh, S. and Bhunia, G.S. (2022): Introduction to drainage basin dynamics: morphology, landscape and modelling. *Drainage Basin Dynamics: An Introduction to Morphology, Landscape and Modelling*, pp.1-9. https://doi.org/10.1007/978-3-030-79634-1_1
- Taib, H., Hadji, R., Hamed, Y., Gentilucci, M. and Badri, K. (2024): Integrated geospatial analysis for identifying regions of active tectonics in the Saharian Atlas, an review analysis of methodology and calculation fundamentals. *Journal of African Earth Sciences*, 211, p.105188. <https://doi.org/10.1016/j.jafrearsci.2024.105188>
- Tandon, S.K. and Sinha, R. (2022): Geology of large river systems. *Large Rivers: Geomorphology and Management, Second Edition*, pp.7-41. <https://doi.org/10.1002/9781119412632.ch2>
- Tesson, J., Benedetti, L., Godard, V., Novaes, C. and Fleury, J. (2021): Slip rate determined from cosmogenic nuclides on normal-fault facets. *Geology* 49, 66–70. doi:10.1130/G47644.1.
- Tucker, G., Hobley, D., McCoy, S. and Struble, W. (2020): Modelling the shape and evolution of normal-fault facets, *J. Geophys. Res.-Earth*, 125, 1–20, <https://doi.org/10.1029/2019JF005305>.

- Turowski, J.M., (2018). Alluvial cover controlling the width, slope and sinuosity of bedrock channels. *Earth Surface Dynamics*, 6(1), pp.29-48. <https://doi.org/10.5194/esurf-6-29-2018>
- Wang, X., Liu, S., Li, Z., Sun, J., Fang, W. and Wang, J. (2024): Implication of alluvial valley width-to-depth ratio on the effect of rock uplift. *Environmental Earth Sciences*, 83(13), p.409. <https://doi.org/10.1007/s12665-024-11714-y>.